ISSN 1674-1056
http://cpb.iphy.ac.cn
http://iopscience.iop.org/cpb
中国物理 B
Chinese Physics
中国物理 Chinese Physics B

Low-threshold bistable reflection assisted by oscillating wave interaction with Kerr nonlinear medium

Yingcong Zhang(张颖聪), Wenjuan Cai(蔡文娟), Xianping Wang(王贤平), Wen Yuan(袁文), Cheng Yin(殷澄), Jun Li(李俊), Haimei Luo(罗海梅), and Minghuang Sang(桑明煌)

Citation: Chin. Phys. B, 2021, 30 (**8**): 084203. DOI: 10.1088/1674-1056/abe118
Journal homepage: http://cpb.iphy.ac.cn; http://iopscience.iop.org/cpb

What follows is a list of articles you may be interested in

Electro-optomechanical switch via tunable bistability and four-wave mixing

Kamran Ullah
Chin. Phys. B, 2019, 28 (**11**): 114209. DOI: 10.1088/1674-1056/ab4580

Controllable optical bistability in a three-mode optomechanical system with a membrane resonator

Jiakai Yan(闫甲楷), Xiaofei Zhu(朱小霏), Bin Chen(陈彬)
Chin. Phys. B, 2018, 27 (**7**): 074214. DOI: 10.1088/1674-1056/27/7/074214

High contrast all-optical diode based on direction-dependent optical bistability within asymmetric ring cavity

Xiu-Wen Xia(夏秀文), Xin-Qin Zhang(张新琴), Jing-Ping Xu(许静平), Ya-Ping Yang(羊亚平)
Chin. Phys. B, 2016, 25 (**8**): 084211. DOI: 10.1088/1674-1056/25/8/084211

Optical bistability and multistability via double dark resonance in graphene nanostructure

Seyyed Hossein Asadpour, G Solookinejad, M Panahi, E Ahmadi Sangachin
Chin. Phys. B, 2016, 25 (**6**): 064201. DOI: 10.1088/1674-1056/25/6/064201

Optical bistability and multistability in a defect slab doped by GaAs/AlGaAs multiple quantum wells

Seyyed Hossein Asadpour, G Solookinejad, M Panahi, E Ahmadi Sangachin
Chin. Phys. B, 2016, 25 (**5**): 054208. DOI: 10.1088/1674-1056/25/5/054208

Low-threshold bistable reflection assisted by oscillating wave interaction with Kerr nonlinear medium*

Yingcong Zhang(张颖聪)[1], Wenjuan Cai(蔡文娟)[1], Xianping Wang(王贤平)[1,2,†], Wen Yuan(袁文)[1], Cheng Yin(殷澄)[3], Jun Li(李俊)[4], Haimei Luo(罗海梅)[1], and Minghuang Sang(桑明煌)[1]

[1] *Jiangxi Key Laboratory of Photoelectronics and Telecommunication, Department of Physics, Jiangxi Normal University, Nanchang 330022, China*
[2] *State Key Laboratory of Advanced Optical Communication Systems and Networks, Shanghai Jiao Tong University, Shanghai 200240, China*
[3] *Jiangsu Key Laboratory of Power Transmission and Distribution Equipment Technology, Hohai University, Changzhou 213022, China*
[4] *Department of Physics, Jiangxi Normal University Science and Technology College, Nanchang 330022, China*

(Received 6 January 2021; revised manuscript received 21 January 2021; accepted manuscript online 29 January 2021)

Owing to the enormously enhanced oscillating wave, a minute variation of the incident light intensity will give rise to a change in the dielectric constant of the Kerr nonlinear medium and lead to a bistable reflection with an ultra-low threshold intensity, which is closely related to the angle of incidence and the thickness of the Kerr nonlinear medium. The criterion for the existence of optical bistability is derived. Our bistability scheme is simple and not limited to the TM-polarization.

Keywords: optical bistability, waveguide, nonlinear optics, Kerr nonlinear material

PACS: 42.79.Gn, 42.65.Pc **DOI:** 10.1088/1674-1056/abe118

1. Introduction

Optical bistability, which is characterized by an S-shaped hysteresis loop, allows two stable outputs for one single input and offers many intriguing applications, such as all-optical switchings,[1,2] optical memories,[3] and optical diodes.[4] There are two critical factors to realize the bistability, one is a resonant behavior and the other is positive feedback. To satisfy the latter critical factor, various proposed schemes draw support from the external stimuli, including the electro-optic effect,[5] and the magneto-optic effect.[6] In contrast, the all-optical bistability is an internal stimulus scheme, where an absorbed or a Kerr nonlinear medium is utilized, and therefore the electronic bottleneck can be excellently avoided. Unfortunately, the needing for an extremely high incident light intensity is hard to solve. For reducing the all-optical bistability threshold intensity, new materials have been synthesized to possess a high Kerr nonlinear coefficient,[7] or the light-matter interaction is enhanced by using the field enhancement effect in the photonic crystal micro-cavities,[8,9] the Fabry–Pérot (FP) resonators,[10,11] fiber Bragg grating cavity,[12–14] and the surface plasmon resonance (SPR).[15–17] Among them, the SPR is a relatively simple approach, however, only the TM polarization mode can be supported.

By extending the guiding layer to a millimeter scale, the symmetrical metal-cladding waveguide (SMCW) is capable of exciting the polarization-independent[18] ultra-high order modes (UHMs), which are highly sensitive to the variation of structural parameters[19] or material constant.[20] Moreover, the enormously enhanced oscillating wave in the guiding layer has been demonstrated such that it can enhance the light-matter interaction, e.g., the Raman scattering,[21,22] the optical trapping,[23] and the RGB lasing.[24] Based on the oscillating wave field enhancement effect, an SMCW structure with a Kerr nonlinear medium inside the guiding layer is proposed to realize the all-optical bistability with an ultra-low hysteresis loop threshold intensity. Compared with the SPR approach, our bistability scheme is no longer limited to the TM-polarization. In addition, to optimize the angle of incident, the criterion of the optical bistability is deduced and discussed in this paper.

2. Structure and principles

The schematic of an SMCW structure, whose guiding layer is composed of a Kerr nonlinear medium and a glass layer, is illustrated in Fig. 1. The guiding layer is sandwiched by a thin metal film on the top side and another thick metal substrate underneath. From top to bottom, their thicknesses are denoted as $h_3 = 45$ nm, $h_2 = 10$ μm, $h_1 = 0.5$ mm and $h_0 = 300$ nm, respectively. For the Kerr nonlinear medium, its dielectric constant is dependent on electric field intensity and can be written as

$$\varepsilon_2 = \varepsilon_2^l + \chi^{(3)} |E|^2, \tag{1}$$

*Projected supported by the Open Fund by State Key Laboratory of Advanced Optical Communication Systems and Networks (Grant No. 2017GZKF18), the National Natural Science Foundation of China (Grant Nos. 12064017, 61765008, 11764020, 11864017, 11804133, and 51567011), the Jiangxi Provincial Natural Science Foundation (Grant No. 20181BAB206034), the Fundamental Research Funds for the Central Universities of China (Grant No. 2017B14914), the Postdoctoral Science Foundation of China (Grant No. 2016M601586), the Science and Technology Project of Changzhou (Grant No. CJ20180048), and Scientific Research Fund of Jiangxi Provincial Education Department (Grant Nos. GJJ150313, GJJ160273, and GJJ170184).

†Corresponding author. E-mail: xpwangphysics@gmail.com

© 2021 Chinese Physical Society and IOP Publishing Ltd

where ε_2^l, $\chi^{(3)}$ and E are the linear part of dielectric constant, the Kerr nonlinear coefficient and the electric field intensity in the Kerr nonlinear medium, respectively. As an example, their values are set to be $\varepsilon_2^l = 2.4025$ and $\chi^{(3)} = 4.4 \times 10^{-17}$ m^2/V^2 [polyDCHD-HS (Ref. [25])]. Both metal films are supposed to be silver, whose dielectric constant ($\varepsilon_3 = -57.8 + \mathrm{i}0.6$ at $\lambda = 1.06$ μm) can be deduced from the Drude model. The dielectric constant of air and the glass are labeled as $\varepsilon_4 = 1$ and $\varepsilon_1 = 2.25$, respectively.

According to the Helmholtz equation,[26] the distribution of the transverse electric (TE) field in each layer of the SMCW can be described as follows:

$$E_y(x) = \begin{cases} A_4 \exp[-\alpha_4(x-h_3)] + B_4 \exp[\alpha_4(x-h_3)], & h_3 < x < +\infty, \\ A_3 \exp(-\alpha_3 x) + B_3 \exp(\alpha_3 x), & 0 < x < h_3, \\ A_2 \exp(-\alpha_2 x) + B_2 \exp(\alpha_2 x), & -h_2 < x < 0, \\ A_1 \exp[-\alpha_1(x+h_2)] + B_1 \exp[\alpha_1(x+h_2)], & -h_1 - h_2 < x < -h_2, \\ A_0 \exp[\alpha_0(x+h_1+h_2)], & -\infty < x < -h_1 - h_2, \end{cases} \tag{2}$$

where A_i and B_i are the electric amplitudes of the plane waves traveling upward and downward, $\alpha_i = \sqrt{\beta^2 - k_0^2 \varepsilon_i}$ is the attenuation coefficient, β is the propagation constant along the Z direction, and $k_0 = 2\pi/\lambda$ is the vacuum wave vector.

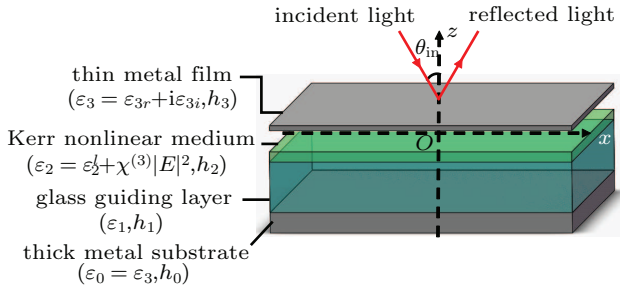


Fig. 1. Schematic of SMCW inserted with a Kerr nonlinear medium in the guiding layer.

Because ε_2 depends on the electric field intensity E_2 in the Kerr nonlinear medium, therefore all the values of A_i' and B_i' can be calculated from a given E_2 based on the boundary continuity conditions, and the prime denotes the initial condition of supposing $A_0' = 1$ in the thick metal substrate. The electric field in the Kerr nonlinear medium is an oscillating wave, thus its electric field intensity E_2' can be written as

$$E_2' = \sqrt{A_2'^2 + B_2'^2}/\sqrt{2}, \tag{3}$$

which is different from the given E_2 since the actual A_0 in the thick metal substrate is not equal to 1. Therefore, the actual A_0 can be re-determined as the ratio E_2/E_2', and then all values of A_i and B_i can be re-calculated from this newly determined A_0. The reflection coefficient is[27]

$$r = \frac{B_4}{A_4} = \frac{r_{43} + r_{3210}\exp(-2\alpha_3 h_3)}{1 + r_{43} r_{3210} \exp(-2\alpha_3 h_3)}, \tag{4}$$

where

$$r_{3210} = \frac{r_{32} + r_{32} r_{21} r_{10} \exp(-2\alpha_1 h_1) + [r_{21} + r_{10}\exp(-2\alpha_1 h_1)]\exp(-2\alpha_2 h_2)}{1 + r_{21} r_{10} \exp(-2\alpha_1 h_1) + r_{32}[r_{21} + r_{10}\exp(-2\alpha_1 h_1)]\exp(-2\alpha_2 h_2)}, \quad r_{ij} = \frac{\alpha_i + \alpha_j}{\alpha_i - \alpha_j}$$

is the Fresnel reflection coefficient at each interface and the subscripts $i, j = 0, 1, 2, 3, 4$, refer to the thick metal substrate, glass guiding layer, Kerr nonlinear medium, thin metal film, and air, respectively. The reflectivity is given by $R = |r|^2$. Furthermore, the light intensity in the Kerr nonlinear medium (I_{Kerr}), the incident light intensity (I_{in}) and the reflected light intensity (I_{r}) are expressed as[28]

$$I_{\mathrm{Kerr}} = \frac{1}{2}\varepsilon_0 c n_2 |E_2|^2, \tag{5}$$

$$I_{\mathrm{in}} = \frac{1}{2}\varepsilon_0 c n_4 |A_4|^2, \tag{6}$$

$$I_{\mathrm{r}} = \frac{1}{2}\varepsilon_0 c n_4 |B_4|^2, \tag{7}$$

where ε_0 and c are the dielectric constant and the speed of light in vacuum, and n_i is the refractive index in the ith layer of the SMCW. Because the guiding layer is coated by two metal films, the excited ultrahigh-order mode propagates in z direction in the guiding layer, leading to the oscillating periodic-distributed electromagnetic energy along the z axis, where the period is determined by the propagation constant, β, of the excited mode.[29] Therefore, the oscillating wave field in the Kerr nonlinear medium is greatly enhanced with respect to the incident light intensity. The amplify factor is defined as

$$A_p = I_{\mathrm{Kerr}}/I_{\mathrm{in}}, \tag{8}$$

which can reach up to 100 and is the core reason for the SMCW enabling an ultra-low threshold intensity. The characteristic equation for a four-layer SMCW can be expressed as[30]

$$\kappa_2 h_2 = m\pi + \arctan\left(\frac{\alpha_3}{\kappa_2}\right) + \arctan\left\{\frac{\kappa_1}{\kappa_2}\tan\left[\arctan\left(\frac{\alpha_3}{\kappa_1}\right) - \kappa_1 h_1\right]\right\}, \tag{9}$$

where $\kappa_i = \sqrt{k_0^2\varepsilon_i - \beta^2}$ are the transverse wavenumbers in the air gap and m is the mode order. In this structure, the thickness of the guiding layer is extended to submillimeter scale, which enables the mode order to reach much larger than 1000. Thus, the polarized-dependent terms can be disregarded, due to the fact that their value is much less than $m\pi$. Here the TE polarization is selected to perform the calculation and simulation, and the analytical procedure of the transverse magnetic (TM) mode is quite similar.

3. Results and discussion

Firstly both materials inside the guiding layer are supposed to be linear. There are several reflection dips with an extremely small full width at half maximum (FWHM) in the reflectivity spectrum (see Fig. 2(a)) and each one corresponds with an ultra-high order mode, which is highly sensitive to the variation in the material constant. To reveal the high sensitivity, one selected reflection dip ($\theta_r = 5.962°$) is enlarged in Fig. 2(b). It indicates that an increment in the dielectric constant of the Kerr nonlinear medium from 2.4025 to 2.4035 with a step of 0.0005 would lead to an obvious right shift of the resonant angle. Moreover, the resonant angle θ_r has a significant linear correlation with the dielectric constant ε_2, i.e., $\theta_r \propto \varepsilon_2$ (not shown in the figure), while the shape of the reflection dip curve changes little. Consequently, if the angle of incidence is fixed at $\theta_{in} = 5.965°$, the reflectivity is initially high (see point A, green star), then jumps to low (see point B, red star), and finally raises back to high again (see point C, blue star).

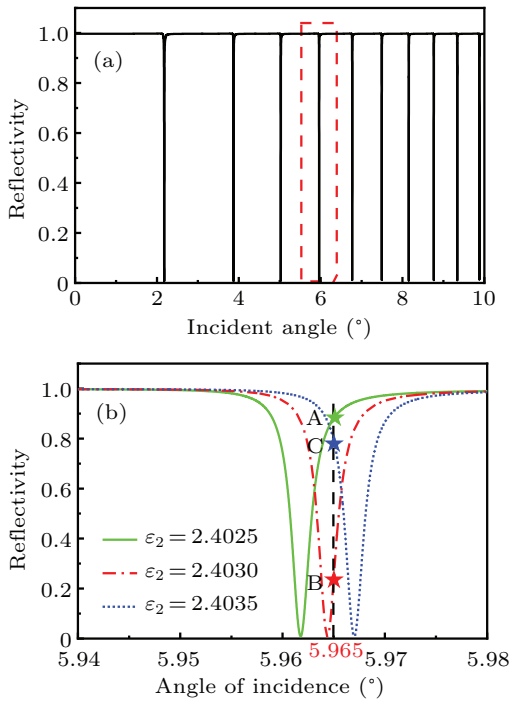


Fig. 2. (a) The reflectivity spectrum of the SMCW with both linear mediums in the guiding layer, (b) reflectivity of one selected reflection dip with different dielectric constant ε_2.

As given in Eq. (2), the light coupled into the guiding layer is guided laterally in the form of an oscillating wave field instead of the evanescent field. The dependence of the amplify factor A_p on the angle of incidence for the selected reflection dip is shown in Fig. 3(a). The maximum value of A_p over 100 can be obtained when the angle of incidence gets close to the resonant angle. Once the resonant condition is slightly dissatisfied, the incident light intensity is almost totally reflected and the amplify factor A_p decreases dramatically. Since the metal substrate is thick enough to prevent the light transmission, the absorption can be simplified to $A = 1 - R$. Figure 3(b) shows the dependence of absorption on the angle of incidence (see black circle). It reveals that there is a good linear relationship between the amplify factor A_p and the absorption A, namely,

$$A_p = bA, \tag{10}$$

where $b = 105.16$ is the linear fitting parameter.

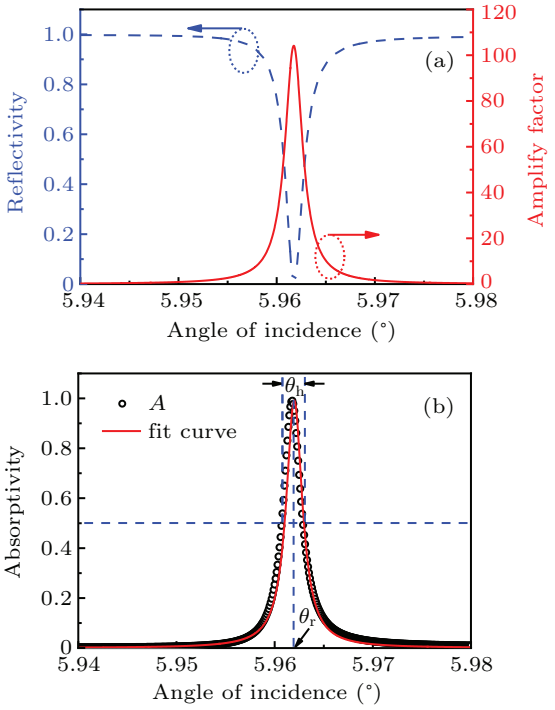


Fig. 3. (a) Amplify factor A_p as a function of the angle of incidence. (b) Absorption (black circle) and its Lorentz fitting curve (red curve) as a function of angle of incidence, where the resonant angle θ_r and the FWHM of absorption peak θ_h are 5.962° and 0.002°, respectively.

When the Kerr nonlinear medium is inserted into the guiding layer, there exists an S-shape curve of the relationship between the reflected light intensity and the incident light intensity. To explain the origin of the bistable reflection, the reflectivity as a function of the angle of incidence is also shown in Fig. 4(a). The initial angle offset is set as $\Delta\theta = \theta_{in} - \theta_r = 0.003°$, where $\theta_{in} = 5.965°$ is the fixed angle of incidence and $\theta_r = 5.962°$ is the resonant angle corresponding to the initial state that the incident light intensity is zero. At the beginning, $\theta_{in} = 5.965°$ locates at the reflection dip's right edge, where

the reflectivity is extremely high and therefore a tiny fraction of incident light intensity is coupled into the Kerr nonlinear medium. Consequently, the reflected light intensity increases approximately linear with the increasing incident light intensity along the upper branch curve because the dielectric constant ε_2 and the reflectivity remain almost unchanged. However, if the incident light intensity exceeds the high threshold intensity I_h (point B), the reflected light intensity suddenly jumps to a small value (point C). Physically, the down-switch phenomenon can be understood as follows: an increment in the incident light intensity increases the electric field intensity in the Kerr nonlinear medium and then the dielectric constant ε_2, which serves to move the resonant angle in the direction of the angle of incidence and to obtain a larger amplify factor A_p in the Kerr nonlinear medium. Thus, a positive feedback is established to cause the resonant angle to change from 5.963° at point B (see the upper panel in Fig. 4(b)) to 5.966° at point C (see the lower panel in Fig. 4(c)). With further increase in the incident light intensity, the reflected light intensity increases linearly again along the lower branch curve since the fixed angle of incidence $\theta_{in} = 5.965°$ now locates at the reflection dip's left edge. In contrast, with the incident light intensity decreases from point C, the reflected light intensity decreases along the lower branch curve to point D (low threshold intensity I_l), then abruptly switches up to point A and further decreases along the upper branch curve to zero. The underlying physics for the up-switch phenomenon is similar to that of the down-switch.

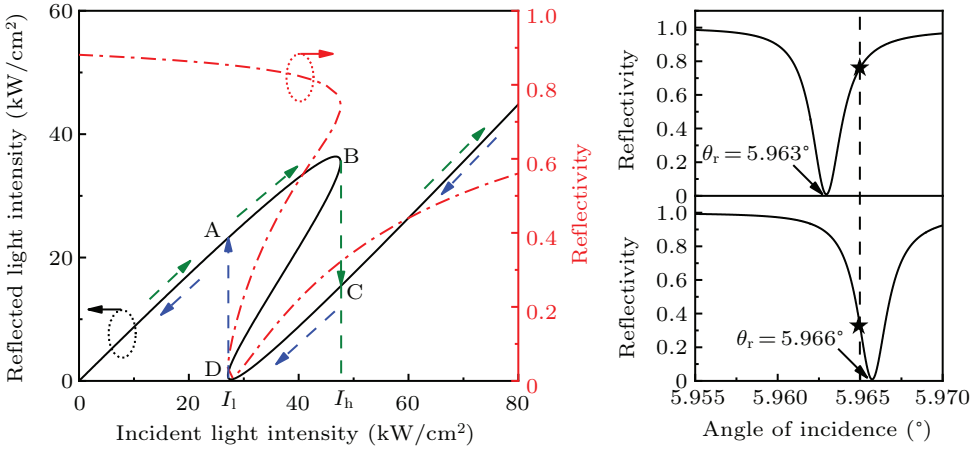


Fig. 4. (a) The reflected light intensity and the reflectivity with respect to the incident light intensity, (b) and (c) the corresponding reflection dips at point B and point C, where the resonant angles are 5.963° and 5.966°, respectively, and the angle of incidence is fixed at $\theta_{in} = 5.965°$.

4. Criterion of optical bistability

In the following, we derive the criterion for the existence of optical bistability. As shown in Fig. 3(b), the absorption can be well approximated by a Lorentz fitting curve (see red curve) with an expression

$$A = \frac{2a}{\pi} \frac{\theta_h}{4(\theta_{in} - \theta_r)^2 + \theta_h^2}, \tag{11}$$

where a is the fitting parameter related to the magnitude of the peak, θ_{in} is the angle of incidence, $\theta_h = 0.002°$ is the FWHM of absorption peak, and $\theta_r = 5.962°$ is the resonant angle.

It has been revealed that the increment in the electric field intensity of the Kerr nonlinear medium I_{Kerr} leads to an increase of the dielectric constant ε_2, which gives rise to a right shift of the reflectivity dip. Combined $\theta_r \propto \varepsilon_2$ with Eqs. (1) and (5), it is found that the resonant angle is also linearly dependent on the electric field intensity in the Kerr nonlinear medium. The expression is

$$\theta_r = \theta_r' + dI_{Kerr}, \tag{12}$$

where θ_r' is the resonant angle for the case $I_{Kerr} = 0$ and d is the fitting parameter. Substituting Eqs. (8), (10) and (12) into Eq. (11), one can obtain

$$I_{in} = \frac{I_{kerr}}{b} \frac{\pi}{2a} \frac{4(\theta_{in} - \theta_r' - dI_{kerr})^2 + \theta_h^2}{\theta_h}. \tag{13}$$

Combined the expression $R = I_r/I_{in}$ with Eqs. (8) and (10), the relationship between the electric field intensity in the Kerr nonlinear medium I_{kerr} and the reflected light intensity I_r can be expressed as

$$I_{kerr} = \frac{bA}{1-A} I_r. \tag{14}$$

By replacing I_{Kerr} in Eq. (14) with I_r, the incident light intensity I_{in} can be described as a cubic function of the reflected light intensity I_r, namely

$$I_{in} = \frac{AI_r}{1-A} \frac{\pi}{2a} \frac{4\left(\theta_{in} - \theta_r' - d\dfrac{AbI_r}{1-A}\right)^2 + \theta_h^2}{\theta_h}. \tag{15}$$

As shown in Fig. 4(a), when optical bistability exists, there must be three values of reflected light intensity I_r corresponding to an incident light intensity I_{in}. Two of them correspond to the upper branch curve and the lower branch curve, respectively, while the middle one is an unstable state. At the down-switch and up-switch positions (see point B and point D in

Fig. 4(a)), the derivative of $I_{\rm in}$ with respect to $I_{\rm r}$ equals zero. Therefore the criterion for the existence of optical bistability is such that the following equation

$$\frac{{\rm d}I_{in}}{{\rm d}I_{\rm r}} = \frac{A}{1-A}\frac{\pi}{2a\theta_{\rm h}}\cdot\left[12\left(\frac{bdA}{1-A}\right)^2 I_{\rm r}^2 - 16(\theta_{\rm in}-\theta_{\rm r}')\frac{bdA}{1-A}I_{\rm r} + 4(\theta_{\rm in}-\theta_{\rm r}')^2+\theta_{\rm h}^2\right] = 0 \tag{16}$$

has two distinct roots, which can be satisfied when $\Delta > 0$. Therefore, one can obtain

$$\left|\theta_{\rm in}-\theta_{\rm r}'\right| > \frac{\sqrt{3}}{2}\theta_{\rm h}. \tag{17}$$

Because the angle of incidence is initially fixed at the right edge of the reflection dip, the criterion for the existence of optical bistability is then written as

$$\theta_{\rm in} > \theta_{\rm r}' + \frac{\sqrt{3}}{2}\theta_{\rm h}. \tag{18}$$

For the selected reflection dip with a resonant angle $\theta_{\rm r}' = 5.962^\circ$ and an FWHM $\theta_{\rm h} = 0.002^\circ$, the angle of incidence must be larger than 5.9637° to obtain the optical bistability.

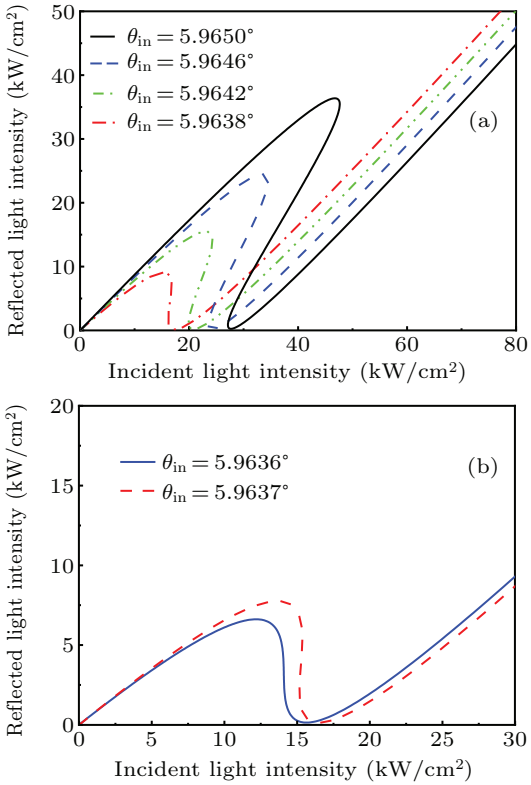


Fig. 5. (a) The S-shaped bistable reflection curves with different angles of incidence, (b) the reflected light intensity with respect to the incident light intensity at two lower angles of incidence ($\theta_{\rm in} = 5.9637^\circ$ and $\theta_{\rm in} = 5.9636^\circ$) to illustrate the criterion for the existence of optical bistability.

The S-shaped bistability reflection curves with a different angle offset $\Delta\theta = \theta_{\rm in} - \theta_{\rm r}'$ have been shown in Fig. 5(a). The incident angle decreases with a step of 0.0004°. The results reveal that both the high threshold intensity $I_{\rm h}$ and low threshold intensity $I_{\rm l}$ decrease with the decrease of the incident. Moreover, the high threshold intensity $I_{\rm h}$ decreases faster than the low threshold intensity $I_{\rm l}$. Thus, the range of the hysteresis loop becomes narrower with reducing the angle offset slightly. In addition, Fig. 5(b) illustrates the situation where the criterion of optical bistability is taken into the consideration. As the incident angle decreases from 5.9637° to 5.9636°, the hysteresis loop initially is obvious and then disappears because the criterion of optical bistability is broken, which agrees to the theoretical calculation (Eq. (18)). As a result, the obtained minimum value for the low threshold intensity $I_{\rm l}$ is 15.16 kW/cm^2 and the high threshold intensity $I_{\rm h}$ is 15.36 kW/cm^2. Compared with the previous results found,[30–32] which are of megawatt scale, our result is much lower. In the simulation process, it is also found that if the angle of incidence is fixed, both the high threshold intensity $I_{\rm h}$ and the low threshold intensity $I_{\rm l}$ also decrease with a thickened Kerr nonlinear medium since the resonant angle shifts to the direction of the angle of incidence (result not shown in the text). Therefore, with this criterion, the ultra-low threshold intensity can be obtained conveniently by optimizing the angle of incidence and the thickness of the Kerr nonlinear medium.

5. Conclusion

In summary, we have presented an SMCW structure which contains a Kerr nonlinear medium in the guiding layer to achieve a bistable reflection with an ultra-low threshold via the oscillating wave field enhancement effect. Owing to the high sensitivity of the excited ultra-high order mode, the threshold intensity is closely related to the angle of incidence and the thickness of the Kerr nonlinear medium. This device could have potential applications in all-optical switch and storage.

References

[1] Zhang W L and Yu S F 2010 *Opt. Commun.* **283** 2622
[2] Guo Q, Zhao X, Zhao H and Chigrinov V 2015 *Opt. Lett.* **40** 2413
[3] Li Y N, Chen Y Y, Wan R G and Yan H W 2019 *Phys. Lett. A* **383** 2248
[4] Xia X, Zhang X, Xu J and Yang Y 2018 *Optik* **167** 95
[5] Witt A, Wegener M, Klingshirn C, Gnass D and Jäger D 1988 *Appl. Phys. Lett.* **52** 342
[6] Umegaki S, Inoue H and Yoshino T 1981 *Appl. Phys. Lett.* **38** 752
[7] Min C, Wang P, Chen C, Deng Y, Lu Y, Ming H, Ning T, Zhou Y and Yang G 2008 *Opt. Lett.* **33** 869
[8] Bravo-Abad J, Rodriguez A, Bermel P, Johnson S, Joannopoulos J and Soljačić M 2007 *Opt. Express* **15** 16161
[9] Wang F Y, Li G X, Tam H L, Cheah K W and Zhu S N 2008 *Appl. Phys. Lett.* **92** 211109
[10] Azadpour F and Bahari A 2019 *Opt. Commun.* **437** 297
[11] Ikeda K and Fainman Y 2006 *Opt. Lett.* **31** 3486
[12] Zang Z G 2013 *Appl. Opt.* **52** 5701
[13] Zang Z G 2012 *Opt. Commun.* **285** 521
[14] Zang Z G and Zhang Y J 2012 *J. Mod. Optic.* **59** 161
[15] Tang S, Zhu B, Xiao S, Shen J and Zhou L 2014 *Opt. Lett.* **39** 3212
[16] Wang G, Lu H, Liu X, Gong Y and Wang L 2011 *Appl. Opt.* **50** 5287
[17] Wysin G, Simon H and Deck R 1981 *Opt. Lett.* **6** 30
[18] Lu H, Cao Z, Li H and Shen Q 2004 *Appl. Phys. Lett.* **85** 4579
[19] Yu T, Li H, Cao Z, Wang Y, Shen Q and He Y 2008 *Opt. Lett.* **33** 1001

[20] Wang X, Yin C, Li H, Sang M, Yuan W and Cao Z 2013 *Opt. Lett.* **38** 4085
[21] Xu T, Huang L, Yin C, Jin Y, Fang J and Huang M 2014 *Appl. Phys. Lett.* **105** 163703
[22] Yin C, Lu Y, Xu T, Wei D Z, Jin Y L, Fang J H, Wang C N and Huang M Z 2016 *J. Raman Spectrosc.* **47** 560
[23] Dai H, Cao Z, Wang Y, Li H, Sang M, Yuan W, Chen F and Chen X 2016 *Sci. Rep.* **6** 32018
[24] Dai H, Yin C, Xiao Z, Cao Z and Chen X 2019 *Phys. Rev. Appl.* **11** 064055
[25] Giorgetti E, Margheri G, Gelli F, Sottini S, Comoretto D, Cravino A, Cuniberti C, Dell'Erba C, Moggio I and Dellepiane G 2001 *Synth. Met.* **116** 129
[26] Rollke K and Sohler W 1977 *IEEE J. Quantum Electron.* **13** 141
[27] Liu X, Cao Z, Zhu P, Shen Q and Liu X 2006 *Phys. Rev. E* **73** 056617
[28] Zhou H, Chen X, Hou P and Li C F 2008 *Opt. Lett.* **33** 1249
[29] Yuan W, Yin C, Xiao P. Wang X, Sun J, Huang S, Chen X and Cao Z 2011 *Microfluid. Nanofluid.* **11** 781
[30] Wang Y, Cao Z Q, Li H G, Hao J, Yu T Y and Shen Q S 2008 *Appl. Phys. Lett.* **93** 091103
[31] Chen J, Wang P, Wang X, Lu Y, Zheng R, Ming H and Zhan Q 2009 *Appl. Phys. Lett.* **94** 081117
[32] Zhang W L and Yu S F 2010 *Opt. Commun.* **283** 2622
[33] Guo J, Jiang L, Jia Y, Dai X, Xiang Y and Fan D 2017 *Opt. Express* **25** 5972